EUROPEAN SOCIETY OF RADIOLOGY
European Radiology

CARDIAC

Quantitative metrics of the LV trabeculated layer by cardiac CT and cardiac MRI in patients with suspected noncompaction cardiomyopathy

Ashish Manohar[1,2,3*], Davis M. Vigneault[2], Deborah H. Kwon[4], Kadir Caliskan[5], Ricardo P. J. Budde[6], Alexander Hirsch[5,6], Seung-Pyo Lee[7], Whal Lee[8], Anjali Owens[9], Harold Litt[10], Francois Haddad[1,3], Gabriel Mistelbauer[2], Matthew Wheeler[1], Daniel Rubin[2,11,12], W. H. Wilson Tang[4] and Koen Nieman[1,2,3*]

Abstract

Objectives To compare cardiac computed tomography (CCT) and cardiac magnetic resonance (CMR) for the quantitative assessment of the left ventricular (LV) trabeculated layer in patients with suspected noncompaction cardiomyopathy (NCCM).

Materials and methods Subjects with LV excessive trabeculation who underwent both CMR and CCT imaging as part of the prospective international multicenter NONCOMPACT clinical study were included. For each subject, short-axis CCT and CMR slices were matched. Four quantitative metrics were estimated: 1D noncompacted-to-compacted ratio (NCC), trabecular-to-myocardial area ratio (TMA), trabecular-to-endocardial cavity area ratio (TCA), and trabecular-to-myocardial volume ratio (TMV). In 20 subjects, end-diastolic and mid-diastolic CCT images were compared for the quantification of the trabeculated layer. Relationships between the metrics were investigated using linear regression models and Bland-Altman analyses.

Results Forty-eight subjects (49.9 ± 12.8 years; 28 female) were included in this study. NCC was moderately correlated ($r = 0.62$), TMA and TMV were strongly correlated ($r = 0.78$ and 0.78), and TCA had excellent correlation ($r = 0.92$) between CMR and CCT, with an underestimation bias from CCT of 0.3 units, and 5.1, 4.8, and 5.4 percent-points for the 4 metrics, respectively. TMA, TCA, and TMV had excellent correlations ($r = 0.93$, 0.96, 0.94) and low biases (−3.8, 0.8, −3.8 percent-points) between the end-diastolic and mid-diastolic CCT images.

Conclusions TMA, TCA, and TMV metrics of the LV trabeculated layer in patients with suspected NCCM demonstrated high concordance between CCT and CMR images. TMA and TCA were highly reproducible and demonstrated minimal differences between mid-diastolic and end-diastolic CCT images.

Clinical relevance statement The results indicate similarity of CCT to CMR for quantifying the LV trabeculated layer, and the small differences in quantification between end-diastole and mid-diastole demonstrate the potential for quantifying the LV trabeculated layer from clinically performed coronary CT angiograms.

*Correspondence:
Ashish Manohar
ashman@stanford.edu
Koen Nieman
knieman@stanford.edu
Full list of author information is available at the end of the article

Springer

Key Points

- *Data on cardiac CT for quantifying the left ventricular trabeculated layer are limited.*
- *Cardiac CT yielded highly reproducible metrics of the left ventricular trabeculated layer that correlated well with metrics defined by cardiac MR.*
- *Cardiac CT appears to be equivalent to cardiac MR for the quantification of the left ventricular trabeculated layer.*

Keywords Cardiomyopathies, Isolated noncompaction of the ventricular myocardium, Computed tomography angiography, Cine MRI, Cardiac imaging techniques

Introduction

Left ventricular (LV) noncompaction, or excessive trabeculation, is characterized by a prominent trabeculated layer within the endocardial LV cavity and a thin compact myocardial layer [1]. It is unclear if this condition exists as a primary cardiomyopathy (noncompaction cardiomyopathy, NCCM), or is an epiphenomenon of either increased cardiac loading conditions, other myocardial disorders, and/or variability in postnatal cardiac development impacted by genetic factors [2, 3]. However, a proportion of patients with LV noncompaction develop heart failure, supraventricular and ventricular arrhythmias, sudden cardiac arrest, and thrombo-embolic events [4].

In clinical practice, echocardiography and cardiac magnetic resonance (CMR) are used to assess the myocardial structure. Several criteria for the classification of LV noncompaction have been established based on the normalized thickness or volume of the trabeculated layer [1]. Cardiac computed tomography (CCT) is an alternative modality to assess the myocardium offering excellent spatial resolution [5]. It may particularly be useful in imaging patients who cannot undergo CMR. Excessive trabeculation may also be suspected on coronary CT angiograms (CCTA) performed for other reasons. CCTA has become an important imaging test to rule out coronary artery disease [6] and the LV trabeculated layer could be quantified from the same CCTA exam without the need for an additional CMR exam. However, data on the performance of CCT for the assessment of LV excessive trabeculation are scarce [7, 8]; specifically, there are no data investigating the quantification of LV excessive trabeculation from mid-diastolic CCT images.

The primary objective of this research work was to study the accuracy and reproducibility of quantitative metrics of the LV trabeculated layer by CCT, using CMR as reference. Because clinical CCT scans are preferably acquired during mid-diastole, a second objective was to assess concordance of quantitative metrics of trabeculation between mid-diastolic and end-diastolic CCT images.

Methods

Study cohort

Study subjects were recruited in the ongoing NON-COMPACT (International Consortium for Multimodality Phenotyping in Adults with Noncompaction) multi-center prospective clinical study (ClinicalTrials.gov: NCT04424030). The primary objective of the NON-COMPACT study is to combine quantitative imaging, genetics, and comprehensive clinical evaluation to predict outcomes in patients with suspected noncompaction cardiomyopathy (NCCM). This study is enrolling subjects ($\geq$18 years of age) with LV excessive trabeculation (as detected on echocardiography images using the Jenni criterion [9]) who underwent CMR for clinical reasons, and of whom a subset also undergoes a research CCT scan. These subjects satisfy only the phenotypic criteria for LV excessive trabeculation, which is one component in the clinical assessment of NCCM. Therefore, these subjects are suspected of having NCCM. The clinical study is conducted across five centers: Stanford University (Stanford, CA, USA), Cleveland Clinic (Cleveland, OH, USA), The Hospital of the University of Pennsylvania (Philadelphia, PA, USA), Erasmus Medical Center (Rotterdam, The Netherlands), and Seoul National University Hospital (Seoul, South Korea). For this research work, 56 consecutively recruited subjects who underwent both CMR and CCT exams within a median interval of 1.4 years were included. Subjects were excluded if either their CMR or their CCT images had severe imaging artifacts that affected the precise estimation of the LV trabeculated layer. The study was approved by the institutional review board at each center (Pro00042745) and all subjects gave written informed consent.

Image acquisition

CCT

Most study subjects ($n=53$) were scanned using 96 detector-row dual-source scanners (SOMATOM Force, Siemens Healthineers), two on a 256 detector-row scanner (Brilliance iCT 256, Philips Healthcare), and one on a 64 detector-row scanner (LightSpeed VCT, General Electric Healthcare).

Contrast-enhanced images were acquired using a prospectively electrocardiogram-triggered axial scan mode without beta-blockers and during inspiratory breath hold. Images with a slice thickness of 0.75 mm (Siemens), 0.8 mm (Philips), or 0.625 mm (GE) were reconstructed using medium sharp kernels (Qr32/Bv36, Siemens; C, Philips; Standard, GE). The median reconstruction field-of-view diameter was 180 mm (interquartile range 162.5–192.5 mm) with a median in-plane pixel spacing of 0.35 mm (interquartile range 0.32–0.38 mm).

CMR

CMR images were acquired using cine balanced steady-state free precession sequences on 1.5-T or 3-T scanners ($n=39$ and 17, respectively): MAGNETOM Aera ($n=6$), MAGNETOM Sola ($n=1$), MAGENTOM SymphonyTim ($n=1$), MAGNETOM Skyra ($n=10$), and MAGNETOM Avanto Fit ($n=1$) (Siemens Healthineers); Achieva ($n=6$) and Ingenia ($n=4$) (Philips Healthcare); and Discovery MR450 ($n=2$), Discovery MR750 ($n=1$), SIGNA Artist ($n=7$), SIGNA Explorer ($n=7$), SIGNA Premier ($n=2$), and SIGNA HDxt ($n=8$) (General Electric Healthcare). The slice thickness was 6 mm ($n=16$) or 8 mm ($n=40$), slice gap was 0 mm ($n=17$), 2 mm ($n=24$), or 4 mm ($n=15$), and the median in-plane pixel spacing was 1.25 mm (interquartile range 0.70–1.44 mm).

Image analysis

Images acquired at the end of diastole were used for the CMR analysis, while images of the mid-diastolic phase were used for the CCT analysis. Datasets for each subject were resampled via cubic interpolation to isotropic pixel (for CMR) and voxel (for CCT) dimensions of 0.5 mm. All primary analyses were performed by the first author (A.M.), a postdoctoral fellow with 8 years of cardiac imaging experience, using custom software developed in MATLAB R2022b (MathWorks, Inc.).

Slice matching between CMR and CCT

For each subject, image slices in the CMR acquired short-axis (SAX) stack that lay below the outflow tract and above the apex were selected for analyses. The first slice in the SAX stack that was completely devoid of the outflow tract was chosen as the basal slice; the last slice in the stack that contained visible LV lumen was chosen as the apical slice. All SAX slices between these two extreme slices were included in the analyses. The median number of SAX slices per subject was 7 (range 4–8).

The volumetric CCT datasets for each patient were rotated into the cardiac coordinate system, with the LV long axis parallel to the z-axis of the scanner. SAX CCT slices (0.5-mm isotropic voxel dimensions) that corresponded to the SAX CMR slices (0.5-mm in-plane pixel dimensions) were selected by visually matching morphological features of the heart.

Contouring and layer definition

Three sets of contours were manually drawn for each of the CMR and CCT slices for each subject:

1. Epicardial contour: drawn at the outer edge of the myocardium.
2. Outer endocardial contour: drawn at the boundary between the contrast-enhanced LV cavity and the myocardium.
3. Inner endocardial contour: drawn within the LV cavity to include only the blood pool, excluding the papillary muscles and the trabeculae.

From these contours, the following three layers were defined for each SAX slice of both the CMR and CCT images (Fig. 1):

1. Compact myocardium (CM): derived by subtracting the area within the outer endocardial contour from the area within the epicardial contour.
2. Trabeculated layer (TL): derived by subtracting the area within the inner endocardial contour from the area within the outer endocardial contour.
3. Non-trabeculated cavity (NTC): defined as the area contained within the inner endocardial contour.

The following two areas were defined for each SAX slice:

$$\textit{Endocardial cavity area} = \mathrm{TL} + \mathrm{NTC}, \tag{1}$$

$$\textit{Myocardial area} = \mathrm{TL} + \mathrm{CM}, \tag{2}$$

To minimize the potential bias of recalling contours, contour tracings in the CMR and CCT images for each subject were performed independently and separated by a minimum of 10 days.

Quantification of the trabeculated layer

In each subject, four metrics were measured from the CCT and CMR images to quantify the trabeculated layer:

1. Noncompacted-to-compacted ratio (*NCC*): defined as the 1D ratio of the maximum thickness of the TL to the thickness of the CM, similar to the "NC/C ratio" described by Jenni et al [9] and Petersen et al [10], but applied to corresponding SAX mid-diastolic CCT and end-diastolic CMR images. From the CMR and CCT image stacks, 3 slices were defined as base, mid, and apex, and subsequently divided into myo-

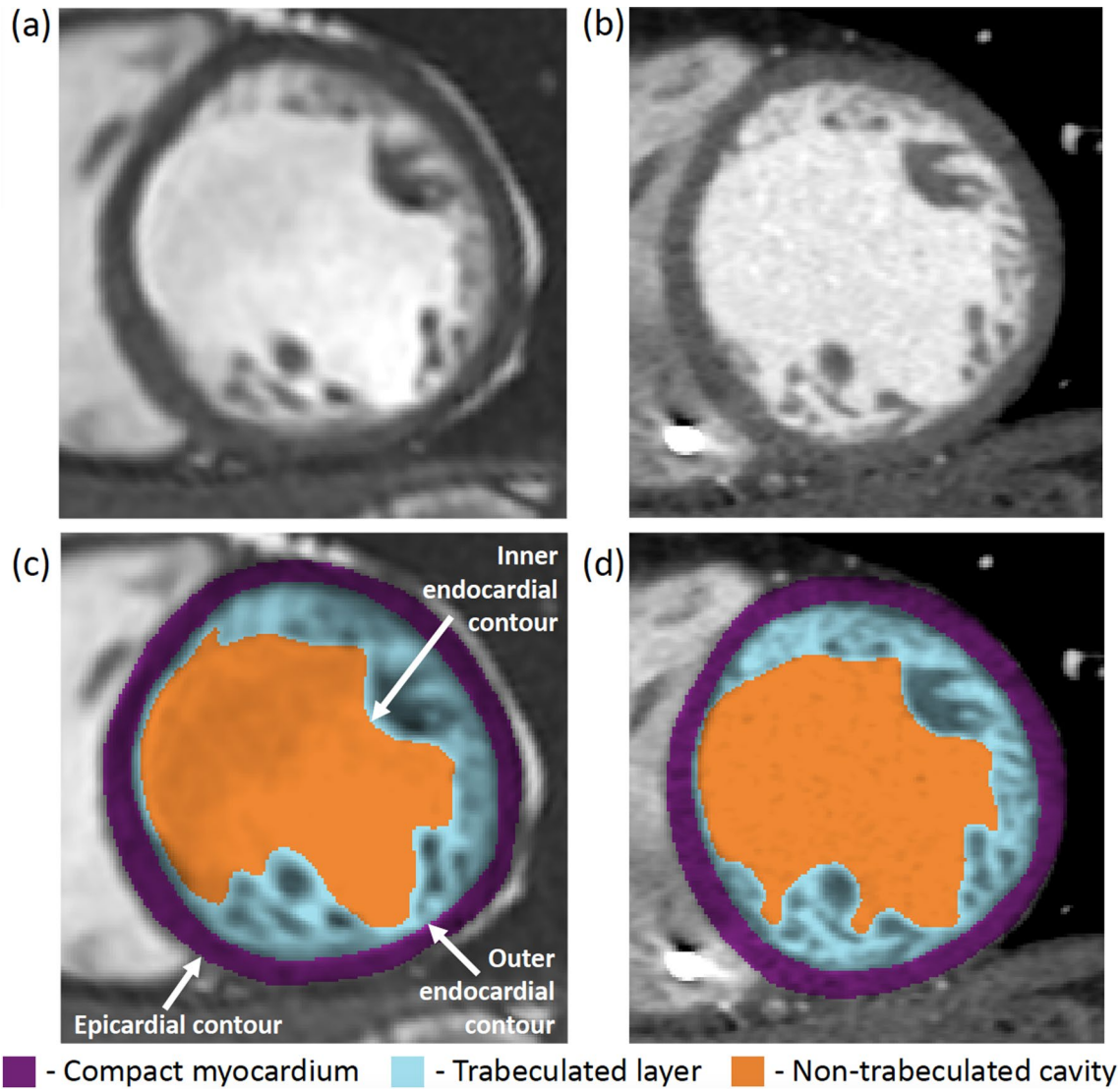

Fig. 1 Layers of the left ventricle. Morphologically matched mid-cavity short-axis slices for (**a**) CMR and (**b**) CCT acquisitions in an example subject. **c**–**d** The three manually delineated layers highlighted in magenta (compact myocardium), cyan (trabeculated layer), and orange (non-trabeculated cavity) for (**c**) CMR and (**d**) CCT. CMR, cardiac magnetic resonance; CCT, cardiac computed tomography

cardial segments in accordance with the American Heart Association's 16-segment model [11]. NCC values were estimated in each of the 16 segments at the region within each segment that visually yielded the highest ratio.

2. Trabecular-to-myocardial area ratio (TMA): defined as the area of the trabeculated layer as a percentage of the myocardial area, similar to that introduced by Jacquier et al [12] but computed as area ratios for each SAX slice. Thus,

$$TMA = \frac{TL}{TL + CM} \times 100, \tag{3}$$

where TL is the trabeculated layer and CM is the compact myocardium.

3. Trabecular-to-endocardial cavity area ratio (TCA): defined as the area of the trabeculated layer as a percentage of the endocardial cavity area. Thus,

$$TCA = \frac{TL}{TL + NTC} \times 100, \tag{4}$$

where NTC is the non-trabeculated cavity. This new metric reflects the extent of trabeculation within the endocardial cavity and was computed for each slice in the SAX stack.

4. Trabecular-to-myocardial volume ratio (TMV): defined as the volume of the trabeculated layer as a percentage of the myocardial volume, as first introduced by Jacquier et al [12]. Thus,

$$\mathrm{TMV} = \frac{\sum_{i=1}^{n} TL_i}{\sum_{i=1}^{n} (TL_i + CM_i)} \times 100, \quad (5)$$

where $i = 1, 2, \ldots, n$ is the slice index within an SAX stack with n slices. This is a global metric for the entire LV.

Comparison between end-diastolic and mid-diastolic CCT phases

Twenty subjects had CCT scans with a wide exposure window, which were used to compare the end-diastolic and mid-diastolic cardiac phases for the quantification of the LV trabeculated layer. The end-diastolic phase was typically acquired using a reduced tube current (20% of the nominal output). A mid-diastolic and an end-diastolic set of five morphologically matched SAX slices ranging from base to apex were selected from the CCT stack, and TMA, TCA, and TMV were estimated for each set.

Reproducibility analysis

Intra- and interobserver reproducibility was tested on imaging studies from 15 randomly selected subjects. For the intraobserver study, the first author who performed the primary analyses repeated the annotation of the CMR and CCT images a minimum of 10 days apart to define the LV layers. For the interobserver study, a diagnostic radiology resident (D.M.V.) with 8 years of cardiac imaging experience independently annotated the CMR and CCT images for the same 15 subjects.

Statistical analysis

Continuous variables were represented as their mean with standard deviation, unless otherwise specified. Categorical variables were expressed as numbers and percentages. Statistically significant differences between groups of continuous and categorical variables were assessed using the two-sample *t*-test and Fisher's exact test, respectively. The maximum NCC value among all 16 AHA segments for each subject was reported for both the CMR and CCT images (Table 1). Linear regression models with Pearson correlation coefficients and Bland-Altman analyses were used to describe the relationships between the CMR- and CCT-derived metrics, as well as the metrics derived from the CCT images of the

Table 1 Subject characteristics

	All subjects ($n = 48$)	Subjects with only mid-diastolic images ($n = 28$)	Subjects with both mid- and end-diastolic images ($n = 20$)	*p* value
Age, years	49.9 ± 12.8	49.9 ± 13.6	49.9 ± 11.9	0.99*
Female, *n* (%)	28 (58)	17 (61)	11 (55)	0.77†
Race, *n* (%)				0.24†
White	31 (65)	20 (71)	11 (55)	
Asian	14 (29)	7 (25)	7 (35)	
Mixed	2 (4)	0 (0)	2 (10)	
Unknown	1 (2)	1 (4)	0 (0)	
Weight, kg	74.9 ± 16.1	77.3 ± 17.3	71.6 ± 14.1	0.24*
Height, cm	171.2 ± 10	172.6 ± 9.9	169.1 ± 10.2	0.25*
Body surface area, m^2	1.9 ± 0.2	1.9 ± 0.2	1.8 ± 0.2	0.21*
LVEF, %	47.6 ± 10.8	48.5 ± 10.9	51.0 ± 9.2	0.46*
CTDIvol, mGy	25 ± 13.6	26.1 ± 16.5	23.5 ± 7.8	0.52*
Time between CMR and CCT exams, median years [IQR]	1.3 [0.2–2.6]	1.2 [0.1–2.3]	1.3 [0.4–2.8]	0.30*
Maximum NCC by CMR	4.3 ± 1.0	4.1 ± 0.9	4.4 ± 1.0	0.37*
Maximum NCC by CCT	3.3 ± 0.9	3.2 ± 0.9	3.4 ± 1.0	0.58*
TMV by CMR, %	51.0 ± 5.2	50.9 ± 5.2	51.2 ± 5.3	0.85*
TMV by CCT, %	46.2 ± 6.2	45.2 ± 5.6	47.6 ± 6.8	0.19*

Data are presented as mean ± standard deviation unless specified otherwise

LVEF left ventricular ejection fraction by echocardiography, *CTDIvol* CT dose index-volume, *IQR* interquartile range, *NCC* noncompacted-to-compacted ratio, *TMV* trabecular-to-myocardial volume ratio, *ED* end-diastole, *MD* mid-diastole

† *p* value computed using Fisher's exact test

* *p* value computed using two-sample *t*-test

end-diastolic and mid-diastolic phases. Pearson correlation coefficients in the range 0.50–0.69, 0.70–0.89, and 0.90–1.00 indicated moderate, strong, and excellent correlations, respectively.

Intra- and interobserver reproducibility of the metrics was assessed by computing intraclass correlation coefficients (ICC) and their 95% confidence intervals using a single rater two-way random effects model with absolute agreement. The same range division as the one used for the Pearson correlation coefficients was used for the ICCs.

Results

Subjects

Of the 56 included subjects, 8 CCT studies had to be excluded due to insufficient image quality: 7 due to low LV contrast and 1 due to severe ICD lead artifacts. Characteristics of the remaining 48 subjects and the subset of subjects with both end-diastolic and mid-diastolic CCT phases are shown in Table 1. The median time interval between the CCT and CMR exams in all 48 subjects was 1.3 years.

Correlation between CMR- and CCT-derived metrics of LV trabeculation

LV excessive trabeculation was detected in 41 and 47 subjects using CCT and CMR, respectively, by applying a threshold of *maximum* NCC > 2.3, which is similar to the Petersen criterion [10] but applied to SAX images rather than LAX images. Furthermore, all 48 subjects satisfied the Jacquier criterion (TMV > 20%) [12] using both CCT and CMR.

Figure 2 shows the relationships between CMR and CCT for the 4 quantitative metrics of the trabeculated layer. Per-segment NCC was moderately correlated ($r = 0.62$; Fig. 2a), TMA ($r = 0.78$; Fig. 2c) and TMV ($r = 0.78$; Fig. 2g) were strongly correlated, and TCA had excellent correlation ($r = 0.92$; Fig. 2e). Additionally, the areas of the compact myocardium had excellent correlation between CMR and CCT (Fig. S1; Supplemental Material). All metrics were statistically different between CMR and CCT ($p < 0.001$).

Comparison between end-diastolic and mid-diastolic CCT phases for the quantification of the LV trabeculated layer

TMA, TCA, and TMV had excellent correlations between the end-diastolic and mid-diastolic CCT images ($r = 0.93$, 0.96, and 0.94, respectively; Fig. 3).

Intra- and interobserver reproducibility

The intra- and interobserver reproducibility of TMA, TCA, and TMV were higher than NCC for both the CMR and CCT images. Specifically, TCA had excellent reproducibility with intra-observer ICC of [0.97, 0.97] and interobserver ICC of [0.88, 0.96] for CCT and CMR, respectively. Table 2 summarizes the results from the reproducibility analyses.

Discussion

The study reveals two primary findings. Firstly, there is a strong correlation between 2D quantitative metrics of the LV trabeculated layer obtained through CCT and those obtained through CMR, with a small underestimation bias by CCT. Secondly, there is a high level of concordance in the metrics between mid-diastolic and end-diastolic CCT images. These results suggest that CCT could be an alternative to CMR for the quantification of the LV trabeculated layer. Additionally, the negligible differences in these metrics between end-diastole and mid-diastole could permit their use on clinical CCTA images acquired during mid-diastole, requiring no dedicated imaging protocols or additional radiation exposure.

Quantification of the LV trabeculated layer with CCT

Echocardiography and CMR are the most commonly performed imaging tests for the evaluation of cardiomyopathies [13]. To the best of our knowledge, this is the first research work to directly compare CMR and CCT for the quantification of the LV trabeculated layer in patients with suspected NCCM [7, 8].

Traditional 1D ratios to quantify noncompaction are observer-dependent [14]; this study confirms this finding, showing modest intra- and inter-observer reproducibility of NCC. 2D (TMA and TCA) and 3D (TMV) metrics of the trabeculated layer were more reproducible for both the CMR and CCT images. TMA, TCA, and TMV

(See figure on next page.)

Fig. 2 Correlation between the CMR- and CCT-derived metrics of the LV trabeculated layer for all subjects. Relationships between CMR- and CCT-derived estimates of (**a**–**b**) NCC, (**c**–**d**) TMA, (**e**–**f**) TCA, and (**g**–**h**) TMV. The left column shows direct correlations between the CMR- and CCT-derived metrics and the right column shows the Bland-Altman analyses. For NCC, each data point corresponds to an American Heart Association segment from one of the 48 subjects. For TMA and TCA, each data point corresponds to a SAX slice from one of the 48 subjects. For TMV, each data point corresponds to one of the 48 subjects. NCC, noncompacted-to-compacted ratio; TMA, trabecular-to-myocardial area ratio; TCA, trabecular-to-endocardial cavity area ratio; TMV, trabecular-to-myocardial volume ratio; MR, metrics derived from cardiac magnetic resonance; CT, metrics derived from cardiac computed tomography; SAX, short-axis slice

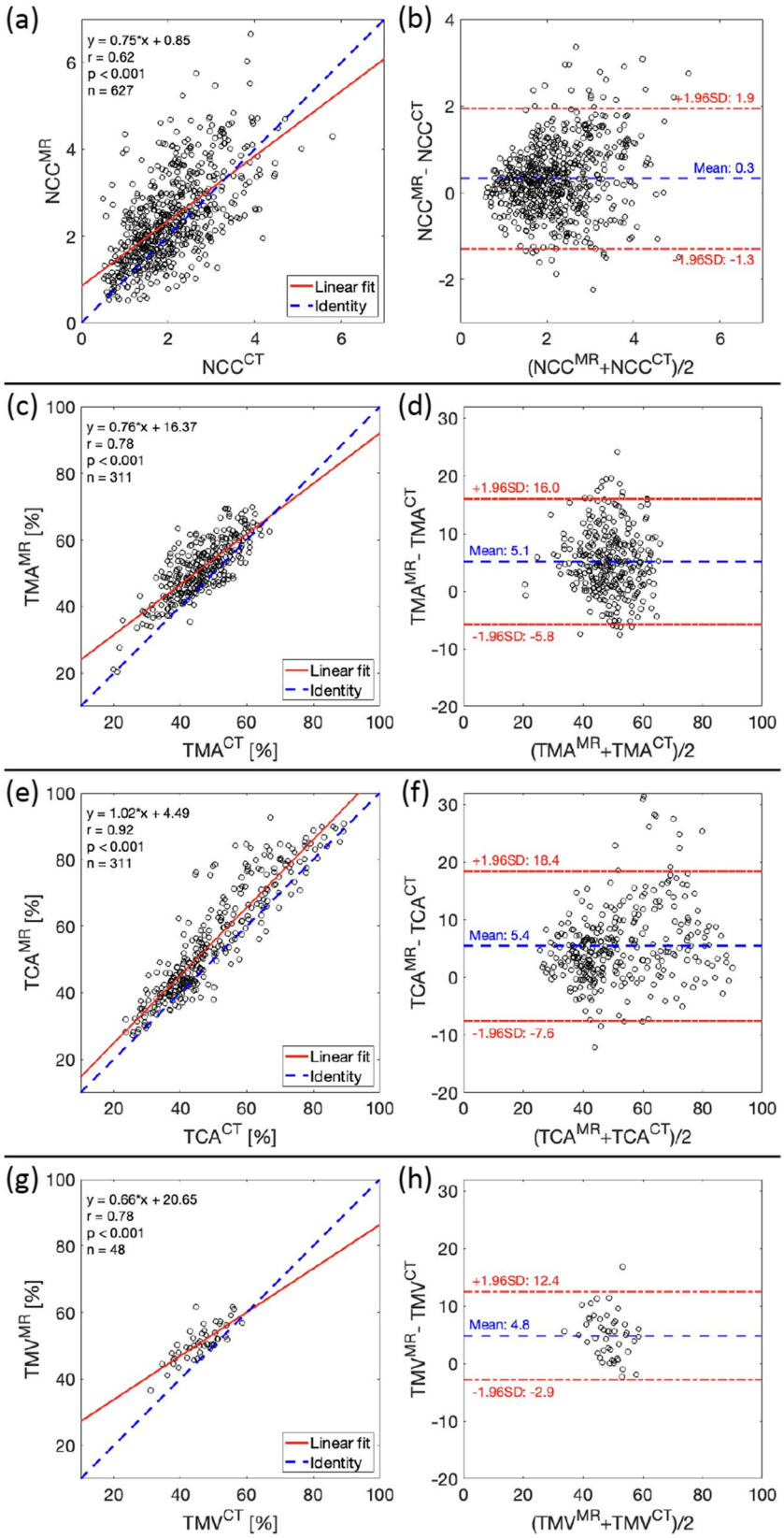

Fig. 2 (See legend on previous page.)

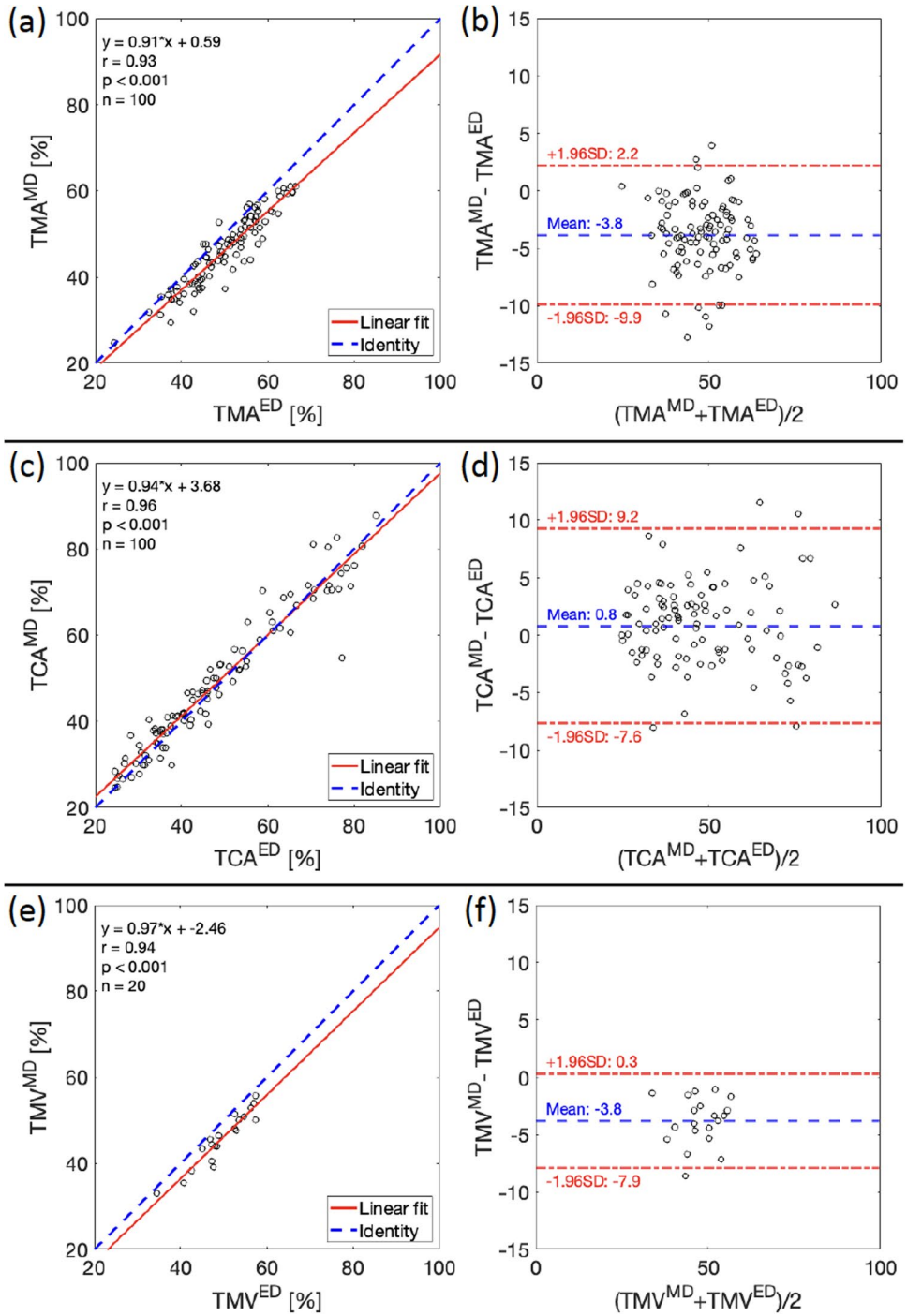

Fig. 3 Comparing end-diastolic and mid-diastolic CCT phases for the quantification of the LV trabeculated layer. Relationships between end-diastolic and mid-diastolic derived estimates of (**a**–**b**) TMA, (**c**–**d**) TCA, and (**e**–**f**) TMV. The left column shows direct correlations between the end-diastolic and mid-diastolic CCT-derived metrics and the right column shows the Bland-Altman analyses. For TMA and TCA, each data point corresponds to a SAX slice from one of the 20 subjects that had multiphase CCT acquisitions. For TMV, each data point corresponds to one of the 20 subjects. ED, end-diastole; MD, mid-diastole; TMA, trabecular-to-myocardial area ratio; TCA, trabecular-to-endocardial cavity area ratio; TMV, trabecular-to-myocardial volume ratio

Table 2 Intra- and interobserver reproducibility analyses

	Intra-observer reproducibility ICC (95% CI)		Interobserver reproducibility ICC (95% CI)	
	CCT	CMR	CCT	CMR
NCC	0.68 (0.60–0.77)	0.79 (0.73–0.85)	0.52 (0.41–0.64)	0.60 (0.49–0.70)
TMA	0.94 (0.92–0.96)	0.90 (0.85–0.96)	0.77 (0.72–0.83)	0.78 (0.70–0.86)
TCA	0.97 (0.96–0.99)	0.97 (0.95–0.98)	0.88 (0.85–0.92)	0.96 (0.94–0.98)
TMV	0.92 (0.86–0.99)	0.94 (0.89–0.98)	0.67 (0.55–0.79)	0.67 (0.44–0.90)

NCC noncompacted-to-compacted ratio, *TMA* trabecular-to-myocardial area ratio, *TCA* trabecular-to-endocardial cavity area ratio, *TMV* trabecular-to-myocardial volume ratio, *ICC* intraclass correlation coefficient, *CI* confidence interval

correlated well between CMR and CCT images; however, the three metrics were lower for CCT. This could be attributed to the following two factors. Firstly, the time delay between the CMR and CCT exams (median interval 1.3 years) may have led to changes in the physical states of the LV, especially considering that all but 7 subjects had their CMR images acquired first. Secondly, it is worth noting that the degree of detail of the inner endocardial contour is observer-dependent and affected by spatial resolution and image quality.

End-diastole vs mid-diastole for the quantification of the LV trabeculated layer

By CMR, the trabecular metrics are measured on end-diastolic images. Because CCT images are typically acquired during the motion-sparse mid-diastolic phase when the LV is not yet at its maximum size, discordance between the two modalities may be introduced. In this study, there was excellent correlation (with small biases) between metrics of the trabeculated layer derived from the end-diastolic and mid-diastolic CCT images. While this observation is encouraging, and would allow for the interpretation of excessive trabeculation on clinical CCT images, discrepancies may vary depending on the pathophysiological state of the heart (atrial fibrillation, atrial flutter, ventricular dysfunction) [15].

Trabecular-to-endocardial cavity area ratio

A new metric that quantifies the trabeculated layer normalized to the endocardial cavity area (TCA) was introduced. Traditionally, excessive trabeculation is quantified as the thickness of the trabeculated layer normalized to the thickness of the myocardium [1]. The rationale for the new TCA metric was to quantify the percentage of the endocardial cavity that comprises the trabeculated layer. More trabeculation within the endocardial cavity could potentially influence cardiac remodeling, increase the intra-ventricular pressure drop, and disrupt cavity hemodynamics [16, 17]. TCA had excellent reproducibility, likely because it depends on the outer endocardial contour, which has the greatest contrast and quantity of landmarks. TMA on the other hand depends on the epicardial contour, which often lacks contrast in many LV segments, making it harder to discern; hence, the higher variability of TMA compared with TCA. Thus, TCA appears to be a promising metric of LV noncompaction, and future work to investigate its clinical value in large multicenter prospective studies is warranted.

Clinical implications and future directions

LV noncompaction remains a poorly understood phenomenon that is detected with increased frequency by advanced imaging techniques [13, 18]. Based on recent pathophysiological insights, the term excessive trabeculation has been introduced [1]. While the debate on appropriate terminology is ongoing [2, 3], both terms have been used interchangeably in this manuscript. The clinical relevance of the findings in this study are that the LV trabeculated layer can be quantified with CCT, and the values are similar to CMR. Additionally, the differences in quantifying the trabeculated layer between the end-diastolic and mid-diastolic CCT images are likely small enough to not be of clinical importance. Excessive trabeculation may thus be detected on CCT images of the chest performed for other indications [19].

Only a limited number of 2D SAX images in the CCT studies were analyzed in order to allow a direct comparison with CMR. However, the full 3D volumetric CCT dataset can also be leveraged to obtain true volumetric information of the trabeculated layer at an unmatched isotropic resolution, as illustrated in Fig. 4, which may provide incremental prognostic information in patients with excessive LV trabeculation.

This work serves as a feasibility study, demonstrating the capability of CCT in quantifying the LV trabeculated layer and detecting LV excessive trabeculation. The encouraging results reported in this study warrant further research to investigate the clinical value of CCT in diagnosing NCCM and predicting adverse cardiac events in this patient population.

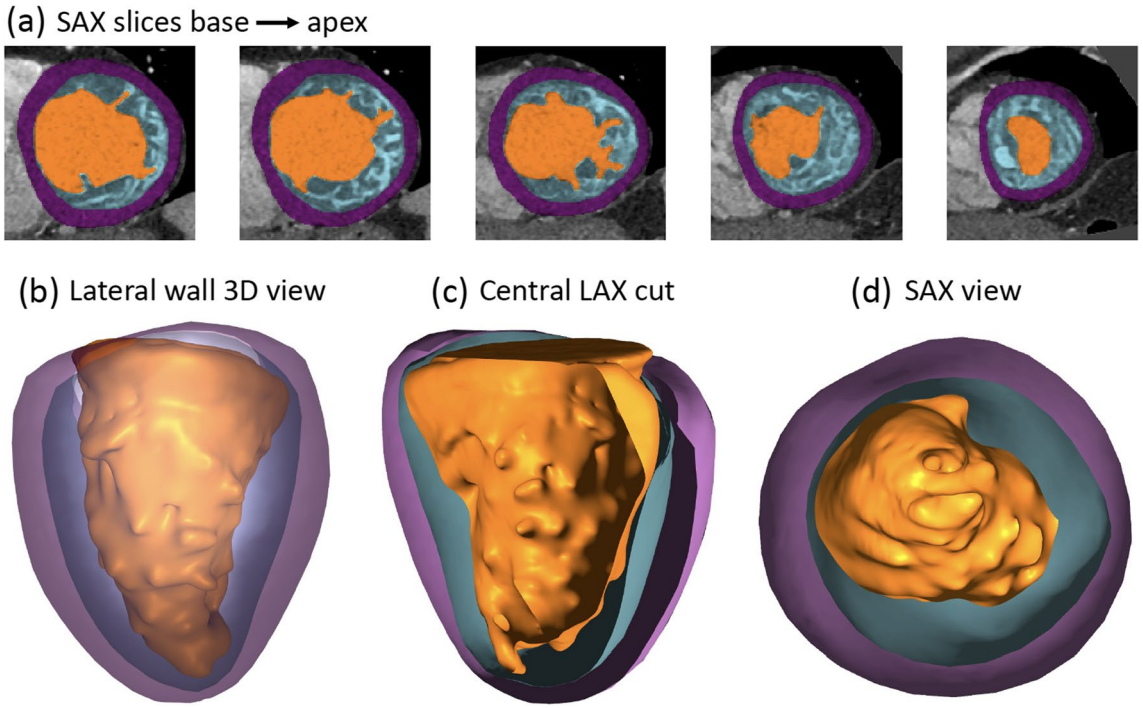

Fig. 4 3D nature of cardiac CT in an example subject. **a** 2D SAX slices from base to apex (left to right) with the compact myocardium (magenta), trabeculated layer (cyan), and non-trabeculated cavity (orange) highlighted. **b**–**d** 3D surface renderings of the epicardial (magenta), outer endocardial (cyan), and inner endocardial (orange) contours represented as a (**b**) 3D view of the lateral wall, (**c**) central LAX cut looking into the non-trabeculated cavity with the lateral wall shown in the background, and (**d**) SAX view looking into the non-trabeculated cavity from the base towards the apex. LAX, long axis; SAX, short axis

Limitations

Subjects with excessive trabeculation that had both CMR and CCT images were included in this work. While this was a unique cohort of subjects, the time interval between the CMR and CCT exams (median interval 1.3 years) may have led to differences in the physical states of the LVs, which could potentially introduce discordance between the two modalities. Additionally, the relationship between CCT and CMR could be affected by the heterogeneity of the CMR scanners.

Despite being the largest cohort of patients with suspected NCCM to have both CMR and CCT acquisitions, the relatively small number of 48 subjects might affect the robustness of the reported correlations.

Out of the 56 subjects, 8 were excluded from the analysis due to CT imaging artifacts. It is important to note that 5 of these 8 subjects that were excluded because of low LV contrast were acquired during the initial stages of the NONCOMPACT study when the CT acquisition protocols were still undergoing active revisions. Therefore, we believe that the exclusion rate in this instance is artificially high and may not be representative of general CT images.

In some cases when the RV lacked contrast, it was difficult to delineate the RV endocardial border of the interventricular septum, and therefore the exact septal thickness in the CCT images. This could be overcome by switching to a 2/3rd phase contrast injection protocol in the future.

The difference in image quality due to dose modulation between the end-diastolic and mid-diastolic phases may have affected the fidelity of the quantification of the LV trabeculated layer; however, despite the differences in image quality, the correlation of these estimates between end-diastole and mid-diastole was excellent with low bias.

This study did not investigate the relationship between end-systolic and end-diastolic CCT-derived quantitative metrics of the LV trabeculated layer. End-systolic CCTA acquisition is currently recommended for high heart rates. Future studies could investigate quantifying the LV trabeculated layer from end-systolic CCT images, potentially demonstrating the versatility and generalizability of CCT.

Lastly, a drawback of CCT is patient exposure to ionizing radiation. However, recent advancements in CT technology now permit the acquisition of high-resolution

3D volumetric images at dose well below 3 mSv [20]. The reduction in X-ray dose will continue to improve with the advent of photon-counting detectors and deep learning reconstructions [21].

Conclusions

In a cohort of 48 subjects with suspected noncompaction cardiomyopathy, CCT-derived metrics of the LV trabeculated layer were highly reproducible and correlated well with those obtained using CMR. Additionally, metrics of the LV trabeculated layer obtained from end-diastolic CCT images had excellent correlation with those estimated from mid-diastolic CCT images. These results suggest that CCT provides similar values to CMR for quantifying the LV trabeculated layer, and the small differences between end-diastole and mid-diastole highlight the potential utility of clinical CCT exams for quantifying the trabeculated layer.

Abbreviations

CCT	Cardiac computed tomography
CCTA	Coronary CT angiography
CM	Compact myocardium
CMR	Cardiac magnetic resonance
ICC	Intraclass correlation coefficient
LV	Left ventricle
NCC	Noncompacted-to-compacted ratio
NCCM	Noncompaction cardiomyopathy
NONCOMPACT	International Consortium for Multimodality Phenotyping in Adults with Noncompaction
NTC	Non-trabeculated cavity
SAX	Short-axis
TCA	Trabecular-to-endocardial cavity area ratio
TL	Trabeculated layer
TMA	Trabecular-to-myocardial area ratio
TMV	Trabecular-to-myocardial volume ratio

Supplementary Information

The online version contains supplementary material available at https://doi.org/10.1007/s00330-023-10526-1.

Below is the link to the electronic supplementary material. Supplementary file1 (PDF 157 KB)

Acknowledgements

The authors would like to thank Aaron Schroeder and Kai Ostendorf for their help in rendering the 3D surfaces of the LV contours.

Funding

This study was funded by the National Institutes of Health (NHLBI R01 HL146754).

Declarations

Guarantor

The scientific guarantor of this publication is Dr. Koen Nieman.

Conflict of interest

Dr. Nieman acknowledges support from the NIH (NIH R01-HL141712; NIH R01-HL146754), and reports unrestricted institutional research support from Siemens Healthineers, Bayer, HeartFlow Inc., and Novartis unrelated to this work, consulting for Novartis and Siemens Medical Solutions USA, and equity in Lumen Therapeutics.
Prof. Budde and Dr. Hirsch acknowledge unrestricted institutional support to Erasmus MC by Siemens Healthineers, Heartflow Inc., and Bayer and lecture fees by Bayer unrelated to this work. Dr. Hirsch also received lecture fees from GE Healthcare unrelated to this work.
Dr. Litt acknowledges unrestricted institutional support to the Perelman School of Medicine of the University of Pennsylvania by Siemens Healthineers and Philips Healthcare for projects unrelated to this work.
Dr. Tang served as consultant for Sequana Medical, Cardiol Therapeutics, Genomics plc, Zehna Therapeutics, Renovacor, WhiteSwell, Kiniksa, Boston Scientific, and CardiaTec Biosciences and has received honorarium from Springer Nature and American Board of Internal Medicine.

Statistics and biometry

No complex statistical methods were necessary for this paper.

Informed consent

Written informed consent was obtained from all subjects in this study.

Ethical approval

Institutional Review Board approval was obtained.

Study subjects or cohort overlap

No study subjects or cohorts have been previously reported.

Methodology

- prospective
- cross-sectional diagnostic study
- multicenter study

Author details

[1]Division of Cardiovascular Medicine, Department of Medicine, Stanford University, Stanford, CA, USA. [2]Department of Radiology, Stanford University, Stanford, CA, USA. [3]Cardiovascular Institute, Stanford University, Stanford, CA, USA. [4]Department of Cardiovascular Medicine, Heart Vascular and Thoracic Institute, Cleveland Clinic, Cleveland, OH, USA. [5]Department of Cardiology, Erasmus University Medical Center, Rotterdam, The Netherlands. [6]Department of Radiology and Nuclear Medicine, Erasmus University Medical Center, Rotterdam, The Netherlands. [7]Department of Internal Medicine, Seoul National University Hospital, Seoul, South Korea. [8]Department of Radiology, Seoul National University Hospital, Seoul, South Korea. [9]Department of Medicine, Division of Cardiology, University of Pennsylvania, Philadelphia, PA, USA. [10]Department of Radiology, University of Pennsylvania, Philadelphia, PA, USA. [11]Department of Biomedical Data Science, Stanford University, Stanford, CA, USA. [12]Division of Biomedical Informatics Research, Department of Medicine, Stanford University, Stanford, CA, USA.

Received: 7 June 2023 Revised: 8 November 2023 Accepted: 29 November 2023
Published online: 19 December 2023

References

1. Petersen SE, Jensen B, Aung N et al (2023) Excessive trabeculation of the left ventricle. JACC Cardiovasc Imaging. https://doi.org/10.1016/j.jcmg.2022.12.026
2. Oechslin E, Jenni R (2017) Nosology of noncompaction cardiomyopathy: the emperor still wears clothes! Can J Cardiol 33:701–704. https://doi.org/10.1016/j.cjca.2017.04.003
3. Anderson RH, Jensen B, Mohun TJ et al (2017) Key questions relating to left ventricular noncompaction cardiomyopathy: is the emperor still wearing any clothes? Can J Cardiol 33:747–757. https://doi.org/10.1016/j.cjca.2017.01.017
4. Oechslin EN, Attenhofer Jost CH, Rojas JR et al (2000) Long-term follow-up of 34 adults with isolated left ventricular noncompaction: a distinct cardiomyopathy with poor prognosis. J Am Coll Cardiol 36:493–500. https://doi.org/10.1016/S0735-1097(00)00755-5

5. Cruz-Bastida JP, Gomez-Cardona D, Li K et al (2016) Hi-Res scan mode in clinical MDCT systems: experimental assessment of spatial resolution performance. Med Phys 43:2399–2409. https://doi.org/10.1118/1.4946816
6. Gulati M, Levy PD, Mukherjee D et al (2021) 2021 AHA/ACC/ASE/CHEST/SAEM/SCCT/SCMR Guideline for the Evaluation and Diagnosis of Chest Pain: A Report of the American College of Cardiology/American Heart Association Joint Committee on Clinical Practice Guidelines. Circulation 144:e368–e454. https://doi.org/10.1161/CIR.0000000000001029
7. Sidhu MS, Uthamalingam S, Ahmed W et al (2014) Defining left ventricular noncompaction using cardiac computed tomography. J Thorac Imaging 29:60. https://doi.org/10.1097/RTI.0b013e31828e9b3d
8. Melendez-Ramirez G, Castillo-Castellon F, Espinola-Zavaleta N et al (2012) Left ventricular noncompaction: a proposal of new diagnostic criteria by multidetector computed tomography. J Cardiovasc Comput Tomogr 6:346–354. https://doi.org/10.1016/j.jcct.2012.07.001
9. Jenni R, Oechslin E, Schneider J et al (2001) Echocardiographic and pathoanatomical characteristics of isolated left ventricular non-compaction: a step towards classification as a distinct cardiomyopathy. Heart 86:666–671. https://doi.org/10.1136/heart.86.6.666
10. Petersen SE, Selvanayagam JB, Wiesmann F et al (2005) Left ventricular non-compaction. J Am Coll Cardiol 46:101–105. https://doi.org/10.1016/j.jacc.2005.03.045
11. Cerqueira MD, Weissman NJ, Dilsizian V et al (2002) Standardized myocardial segmentation and nomenclature for tomographic imaging of the heart. Circulation 105:539–542. https://doi.org/10.1161/hc0402.102975
12. Jacquier A, Thuny F, Jop B et al (2010) Measurement of trabeculated left ventricular mass using cardiac magnetic resonance imaging in the diagnosis of left ventricular non-compaction. Eur Heart J 31:1098–1104. https://doi.org/10.1093/eurheartj/ehp595
13. Ross SB, Jones K, Blanch B et al (2020) A systematic review and meta-analysis of the prevalence of left ventricular non-compaction in adults. Eur Heart J 41:1428–1436. https://doi.org/10.1093/eurheartj/ehz317
14. Saleeb SF, Margossian R, Spencer CT et al (2012) Reproducibility of echocardiographic diagnosis of left ventricular noncompaction. J Am Soc Echocardiogr 25:194–202. https://doi.org/10.1016/j.echo.2011.10.002
15. Namana V, Gupta SS, Sabharwal N, Hollander G (2018) Clinical significance of atrial kick. QJM 111:569–570. https://doi.org/10.1093/qjmed/hcy088
16. Paun B, Bijnens B, Butakoff C (2018) Relationship between the left ventricular size and the amount of trabeculations. Int J Numer Methods Biomed Eng 34:e2939. https://doi.org/10.1002/cnm.2939
17. Sacco F, Paun B, Lehmkuhl O et al (2018) Left ventricular trabeculations decrease the wall shear stress and increase the intra-ventricular pressure drop in CFD simulations. Front Physiol 9:458. https://doi.org/10.3389/fphys.2018.00458
18. Ivanov A, Dabiesingh DS, Bhumireddy GP et al (2017) Prevalence and prognostic significance of left ventricular noncompaction in patients referred for cardiac magnetic resonance imaging. Circ Cardiovasc Imaging 10:e006174. https://doi.org/10.1161/CIRCIMAGING.117.006174
19. Maron DJ, Hochman JS, Reynolds HR et al (2020) Initial invasive or conservative strategy for stable coronary disease. N Engl J Med 382:1395–1407. https://doi.org/10.1056/nejmoa1915922
20. Stocker TJ, Deseive S, Leipsic J et al (2018) Reduction in radiation exposure in cardiovascular computed tomography imaging: results from the PROspective multicenter registry on radiaTion dose Estimates of cardiac CT angIOgraphy iN daily practice in 2017 (PROTECTION VI). Eur Heart J 39:3715–3723. https://doi.org/10.1093/eurheartj/ehy546
21. Lell MM, Kachelrieß M (2020) Recent and upcoming technological developments in computed tomography. Invest Radiol 55:8–19. https://doi.org/10.1097/RLI.0000000000000601

Publisher's Note